



Article

Editor's Choice

# The Earliest Generation of Diamond: The First Find of a Diamond Inclusion in Kimberlitic Olivine

Lyudmila Pokhilenko, Nikolay Pokhilenko, Vladimir Malkovets and Taisia Alifirova

## Special Issue

Kimberlites and Related Rocks: New Insight into Petrogenesis and Diamond Potential of Deeply-Derived Mantle Magmas

Edited by




Dr. Igor Sharygin, Dr. Alexander Golovin, Dr. Dmitry Zedgenizov and Dr. Anna Dymshits



<https://doi.org/10.3390/min13010036>

## Article

# The Earliest Generation of Diamond: The First Find of a Diamond Inclusion in Kimberlitic Olivine

Lyudmila Pokhilenko <sup>1,\*</sup>, Nikolay Pokhilenko <sup>1,2</sup>, Vladimir Malkovets <sup>1,3</sup> and Taisia Alifirova <sup>4</sup><sup>1</sup> Institute of Geology and Mineralogy SB RAS, Novosibirsk 630090, Russia<sup>2</sup> Department of Geology and Geophysics, Novosibirsk State University, Novosibirsk 630090, Russia<sup>3</sup> Vilyuyskaya Geological Exploration Expedition Public Joint Stock Company «ALROSA», Mirny 678174, Republic of Sakha (Yakutia), Russia<sup>4</sup> Department of Lithospheric Research, University of Vienna, 1090 Vienna, Austria

\* Correspondence: blingoreluiy@yandex.ru; Tel.: +7-(913)-717-5391

**Abstract:** Today, it is known that the majority of diamonds are crystallized mostly from a metasomatic agent close in the main characteristics to carbonatite melts acting upon mantle rocks, and therefore, diamonds are located in the interstitial space of these rocks. So far, diamond has never been found included in other kimberlitic or xenolithic minerals. We have found a diamond inclusion inside the kimberlitic olivine grain, which is the first find of its kind. The diamond crystal is to have been captured by the growing olivine at quite high temperatures (more than 1400 °C) early in the history of the cratonic lithospheric mantle formation. The event had taken place long before the depleted peridotite cooled down to the temperature of the Middle Archean cratonic geotherm corresponding to the diamond stability field at depths where carbonatite melts can react with depleted peridotite, making it a diamond-bearing rock. On the one hand, this find provides evidence that diamonds can crystallize from the high-temperature silicate melt with some carbonate component. On the other hand, the diamond was found coexisting with a sulfide inclusion in the same olivine, i.e., crystallization from a sulfide melt may be another way of diamond formation.

**Keywords:** diamond; olivine; sulfide; lithospheric mantle; diamond-forming media; Middle Archean cratonic geotherm



**Citation:** Pokhilenko, L.; Pokhilenko, N.; Malkovets, V.; Alifirova, T. The Earliest Generation of Diamond: The First Find of a Diamond Inclusion in Kimberlitic Olivine. *Minerals* **2023**, *13*, 36. <https://doi.org/10.3390/min13010036>

Academic Editor: Paolo Nimis

Received: 25 November 2022

Revised: 22 December 2022

Accepted: 23 December 2022

Published: 26 December 2022



**Copyright:** © 2022 by the authors. Licensee MDPI, Basel, Switzerland. This article is an open access article distributed under the terms and conditions of the Creative Commons Attribution (CC BY) license (<https://creativecommons.org/licenses/by/4.0/>).

## 1. Introduction

Mantle mineral inclusions in other minerals of mantle origin record different stages of deep-seated rock formation and conditions in the mantle and allow identifying the parageneses of minerals crystallized in different P-T-fO<sub>2</sub> conditions. Diamond is a concentrator of minerals whose compositions reflect a wide range of mantle conditions. Therefore, interest in the study of diamonds and inclusions in diamonds has not subsided for many decades, e.g., [1–8]. Large megacrystals of olivine and garnet grains in diamondiferous xenoliths of megacrystalline peridotites described previously [9–13] are characterized by a developed crack system. All diamonds which were found earlier in these rocks were placed in the cracks (Figure 1). There are some descriptions of garnet megacrysts with diamond crystals sitting on the surface or inside the sample [14–16]. In all the cases, diamond grains were described as placed in the crack systems, and there were evident signs of secondary alteration and partial melting developing inside the cracks [15,16]. There has been no evidence of diamond ever found included in primary olivine, garnet, or pyroxene from the mantle xenoliths or in kimberlitic megacrysts [17]. Three-dimensional X-ray tomography of diamondiferous mantle eclogite xenoliths has convincingly shown that previous finds of eclogitic diamonds enclosed in garnets or pyroxenes are associated with metasomatic veins [18].

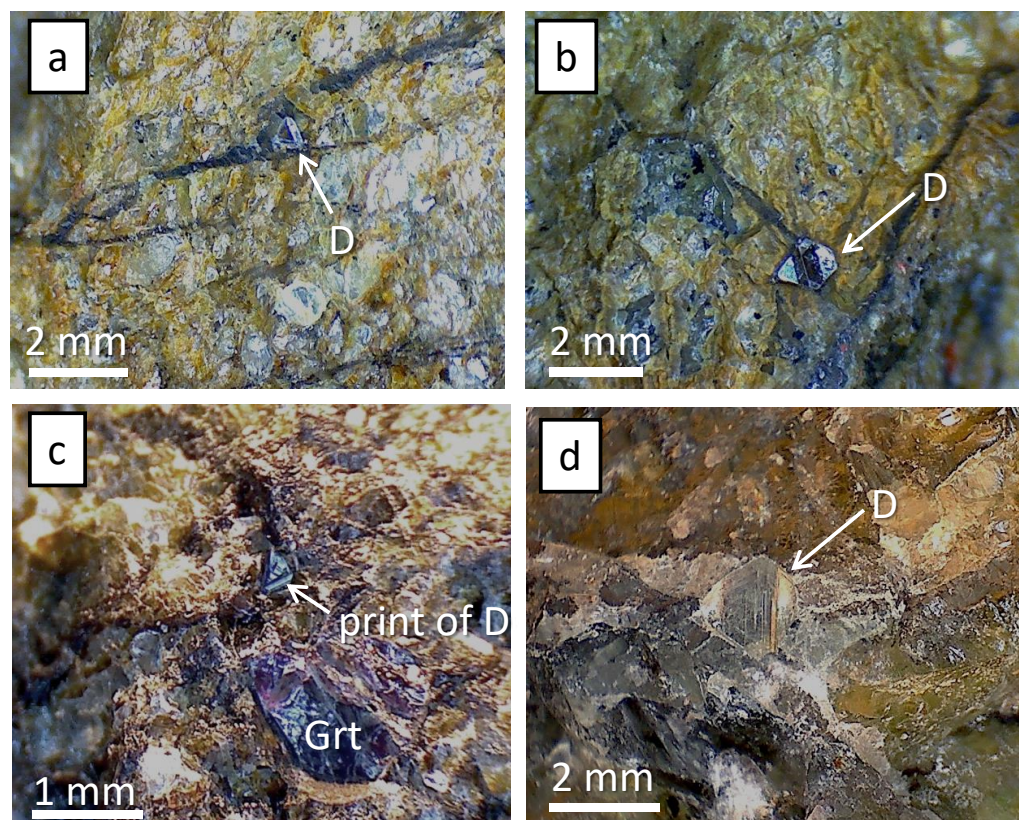


**Figure 1.** Diamonds (d) in the cracks in olivine of megacrystalline dunites from the Udachnaya kimberlite pipe (Yakutia, Russia): (a,b) U-69/76; (c) U-450/89; (d) LUV-833.

Olivine is the main mineral of the depleted mantle and often acts as a host of mineral inclusions. The compositions of mineral inclusions (lherzolite and harzburgite-dunite garnets, clino- and orthopyroxenes, and chromite) in olivine from Udachnaya kimberlite pipe were first characterized in the work of Laz'ko and coauthors [19]. Later, more knowledge became available on both the inclusions and the olivine hosts; namely, olivines of generations I and II were distinguished, and the inclusions were considered in terms of their location in core or rim zones [20]. The list of enclosed minerals was extended later by phlogopite, perovskite, and rutile, as well as the rarer phases of magnetite and magnesian ilmenite in olivine rims. It was emphasized that crystal inclusions in olivine are primary [20]. Diamond inclusions in olivine have never been reported before. Here, we discuss an exceptional find of two almost equally sized crystalline inclusions: diamond and sulfide in a transparent olivine grain from the Udachnaya East kimberlite pipe in Yakutia.

## 2. Materials and Methods

The diamond crystal, the forsteritic matrix, and hydrocarbons were examined using micro-Raman spectroscopy on a Horiba Jobin Yvon LabRAM HR800 microspectrometer (Horiba Ltd., Kyoto, Japan) equipped with a confocal optical system and 532-nm emission laser. Elemental abundances in the olivine matrix and sulfide grain, found as an inclusion in olivine next to the diamond inclusion, were measured by EMPA on a JEOL JXA-8100 electron microprobe (JEOL, Tokyo, Japan) at an acceleration voltage of 20 kV, a focused beam current of 10 nA, and a count time of 20 to 30 s. Detection limits for major oxides in olivine are typically <0.04 wt% for SiO<sub>2</sub> and MgO, <0.05–0.07 wt% for FeO, and 19, 13, and 9 ppm for MnO, Cr<sub>2</sub>O<sub>3</sub>, and CaO, respectively. Detection limits for sulfide are (ppm) 106 for S, 144 for Cr, 63 for Co, 128 for Ni, and 175 for Cu. The quoted contents are for different zones of the studied sulfide. Analysis of olivine sections around the diamond inclusion was performed using TESCAN MIRA3 LMU equipped with Oxford

Instruments INCA-450 at the Analytical Center for multi-elemental and isotope research, SB RAS (Novosibirsk, Russia) and was carried out on the state assignment of IGM SB RAS. The acceleration voltage and counting time were 20 kV and 300 s, respectively. Elemental maps were constructed using a TESCAN scanning electron microscope with a counting time of 1800 s. The Re-Os isotope composition and PGE analyses were performed at the Geochemical Analysis Unit (GAU) at the ARC National Key Centre GEMOC, Macquarie University, Sydney. The in situ Re-Os isotope composition of the sulfide was analyzed using a Merchantek New Wave UV213 laser microprobe (LAM) with a large-format cell, attached to a Nu Plasma multiple collector (MC) ICPMS. All ablations were carried out using He as the carrier gas. The laser operating conditions are 5 Hz frequency, beam energy of 1–2 mJ/pulse, and 80  $\mu\text{m}$  spot size. The overlap of  $^{187}\text{Re}$  on Os was corrected by measuring the  $^{185}\text{Re}$  peak and using  $^{187}\text{Re}/^{185}\text{Re} = 1.6741$ , which has been determined in [21]. The analytical procedures have been described in detail [21]. The PGEs were analyzed using a Merchantek New Wave UV213 laser microprobe (LAM) with a large-format cell, attached to an Agilent 7500 cs quadrupole ICP MS and using methods described by Alard et al. [22]. External standards were a synthetic NiS bead with 200 ppm Os and Pt (PGE-A) and the NIST610 glass standard. Data were reduced using the in-house GLITTER software [23], developed in ARC (The Australian Research Council) National Key Centre GEMOC, Macquarie University, Sydney, Australia. The ARC National Key Centre for Geochemical Evolution and Metallogeny of Continents (GEMOC) is based in the Department of Earth and Planetary Sciences at Macquarie University.

### 3. Results

#### 3.1. Olivine Composition

The olivine grain studied is a  $1.5 \times 1.5 \times 0.5 \text{ cm}^3$  greenish-yellow olivine with a uniform composition (Table 1). According to its morphology and chemistry, it belongs to generation I olivine from the Udachnaya kimberlite described by Kamenetsky et al. [20]. It seems to be the most magnesian one (Fo = 93.1) among the compositionally diverse Udachnaya xenolithic olivines [12,24–26], olivine xenocrysts from South African pipes, and Greenland olivines [27]. Its major- and trace-element chemistry generally corresponds to that of olivine inclusions in diamond [4,5,28–31]; the CaO and MnO contents are within the lowest ranges for such inclusions.

**Table 1.** Composition of the host olivine (wt%).

| N                              | 1–1   | 1–2   | 1–3   | 1–4   | 1–5   | Average |
|--------------------------------|-------|-------|-------|-------|-------|---------|
| SiO <sub>2</sub>               | 42.11 | 42.11 | 41.79 | 41.89 | 41.84 | 41.95   |
| Cr <sub>2</sub> O <sub>3</sub> | 0.045 | 0.046 | 0.045 | 0.049 | 0.046 | 0.046   |
| FeO                            | 6.76  | 6.74  | 6.75  | 6.74  | 6.74  | 6.75    |
| MnO                            | 0.081 | 0.082 | 0.083 | 0.081 | 0.084 | 0.082   |
| MgO                            | 51.31 | 51.21 | 50.94 | 51.12 | 51.04 | 51.12   |
| CaO                            | 0.013 | 0.013 | 0.011 | 0.010 | 0.013 | 0.012   |
| NiO                            | 0.348 | 0.346 | 0.347 | 0.347 | 0.352 | 0.348   |
| Total                          | 100.7 | 100.5 | 99.97 | 100.2 | 100.1 | 100.3   |

Note: EMPA data from JEOL JXA-8100 electron microprobe. Analyzed by V.N. Korolyuk. To check the homogeneity, the studied olivine was analyzed five times in different places (N: 1.1–1.5).

The elemental maps of olivine were made, and olivine sections different in size around the diamond were analyzed. Both maps and chemical analyses demonstrate the homogeneity of olivine in all components (Figure 2, Table 2). Some small pieces of olivine were found near the top of the diamond octahedron. They were placed in the stress crack. These pieces (see No. 4, 5 in Figure 2 and Table 2) are utterly identical in composition to the “main” olivine (see No. 2, 3 in Figure 2 and Table 2), and they cannot be the grains of the late recrystallized olivine. Being associated with the stress crack, they are likely the result of local shear deformation in the olivine crystal.

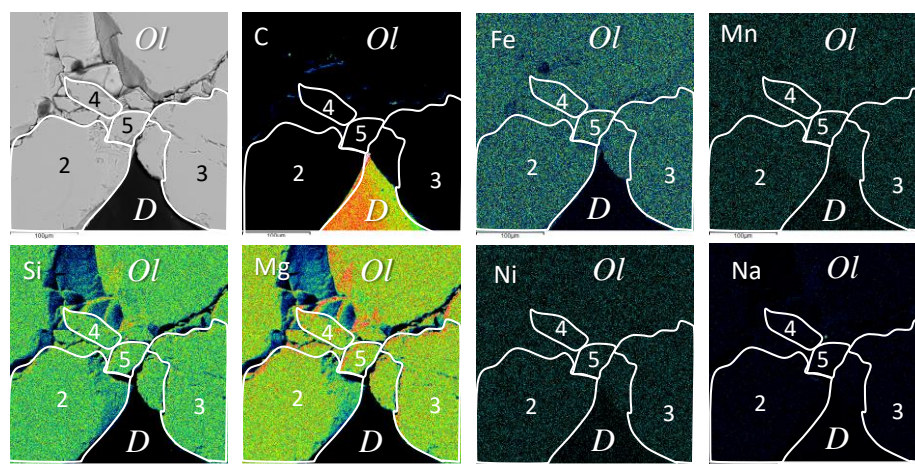


**Figure 2.** Elemental maps of olivine around diamond. The first left picture shows olivine sections around the diamond analyzed using TESCAN: the numbers 2–5 correspond to numbers (N) in Table 2.

**Table 2.** Composition of the olivine around the diamond inclusion (wt%).

| N                              | 2     | 3     | 4     | 5     |
|--------------------------------|-------|-------|-------|-------|
| SiO <sub>2</sub>               | 40.93 | 40.9  | 41.31 | 41.18 |
| Al <sub>2</sub> O <sub>3</sub> | 0.11  | 0.11  | 0.09  | 0.13  |
| Cr <sub>2</sub> O <sub>3</sub> | 0.06  | 0.04  | 0.06  | 0.06  |
| FeO                            | 6.63  | 6.65  | 6.73  | 6.64  |
| MnO                            | 0.08  | 0.09  | 0.09  | 0.05  |
| MgO                            | 51.09 | 51.03 | 51.47 | 51.36 |
| Na <sub>2</sub> O              | 0     | 0.05  | 0.05  | 0.04  |
| NiO                            | 0.38  | 0.39  | 0.39  | 0.39  |
| Total                          | 99.27 | 99.28 | 100.2 | 99.86 |

Note: EDS data from TESCAN scanning electron microscope. Analyzed by M.V. Khestov.

### 3.2. Inclusions Description

The olivine hosts two inclusions spaced at ~3 mm, each surrounded by stress cracks (Figure 3a). One is a colorless transparent octahedron, about 0.3 mm in size (Figure 3b,d). Its crystal morphology and Raman spectra undoubtedly identify it as a diamond (Figure 4, Spectrum a).

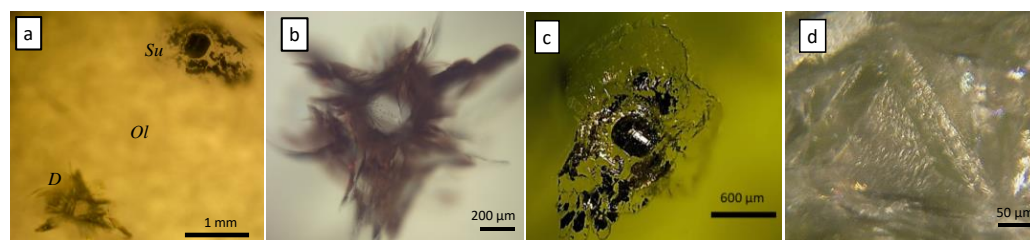


**Figure 3.** Diamond and sulfide inclusions in olivine from the Udachnaya kimberlite (Yakutia): (a) both inclusions; (b) well-defined octahedral morphology of the diamond crystal; (c) sulfide inclusion with a cracking halo; (d) resorbed facet of diamond.

The other inclusion is a sulfide (Figure 3c), isometric, with zones of different colors in the back-scattered electron (BSE) image (Figure 5). It has a discontinuous narrow (5–20 μm) rim of Ni-bearing chalcopyrite (1.09 wt% Ni), a slightly broader (10–25 μm) pentlandite zone of an outer core (with 0.5 to 1.08 wt% Co), and an inhomogeneous inner core of mss with Ni impurity (7.13–10.46 wt%). The inner core is a dark matrix with patches or most often bands, 1 μm wide or narrower, of a lighter-colored material (the color of

the pentlandite zone). Integral analysis of that “mixture-zone” indicates twice-higher Ni contents in comparison with the dark grey zones, which probably reflects the presence of exsolution lamellae (pentlandite in pyrrhotite).

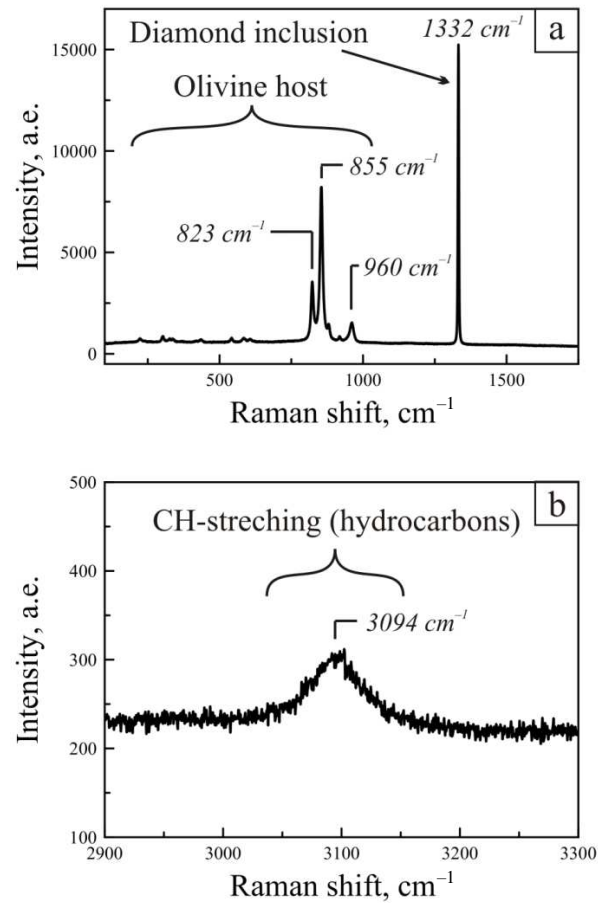


**Figure 4.** Raman spectra of studied sample: (a) spectrum of the forsterite matrix and the diamond inclusion; (b) the mode of aromatic or olefinic compounds on the diamond inclusion interface.

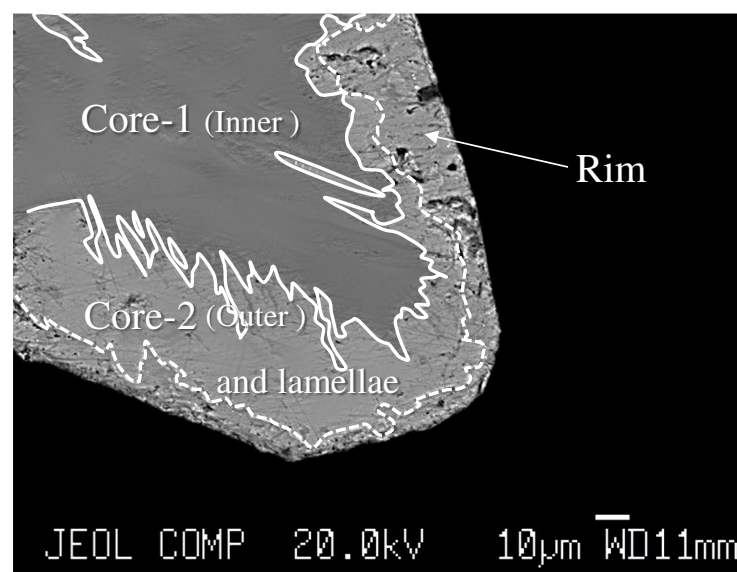


**Figure 5.** Sulfide inclusion in olivine from the Udachnaya kimberlite (Yakutia): BSE image of mss: Core-1 (inner), pentlandite Core-2 (outer), and chalcopyrite rim.

The compositions of the zones are shown in Table 3.

**Table 3.** Composition of the sulfide inclusion.

| wt%   |        | Core-1 (Inner Part)              |        |       |        |        |       |        |        |     |
|-------|--------|----------------------------------|--------|-------|--------|--------|-------|--------|--------|-----|
| N     | 1      | 2                                | 3      | 4     | 5      | 6      | 7     | 8      | 9      |     |
| S     | 39.31  | 39.58                            | 39.20  | 39.15 | 39.30  | 39.49  | 39.75 | 39.24  | 39.22  |     |
| Fe    | 52.50  | 52.62                            | 51.86  | 51.77 | 49.90  | 49.90  | 49.09 | 52.87  | 50.22  |     |
| Cr    | 0.20   | 0.18                             | 0.21   | 0.22  | 0.24   | 0.13   | 0.15  | 0.18   | 0.16   |     |
| Co    | 0.18   | 0.13                             | 0.13   | 0.15  | 0.13   | 0.16   | 0.28  | 0.11   | 0.13   |     |
| Ni    | 7.75   | 7.35                             | 8.04   | 8.03  | 10.46  | 10.37  | 10.02 | 7.13   | 10.09  |     |
| Cu    | 0.02   | 0.00                             | 0.01   | 0.00  | 0.02   | 0.00   | 0.00  | 0.00   | 0.00   |     |
| Total | 99.95  | 99.86                            | 99.45  | 99.32 | 100.04 | 100.05 | 99.29 | 99.53  | 99.83  |     |
| at%   |        | Core-1 (Inner Part)              |        |       |        |        |       |        |        |     |
| N     | 1      | 2                                | 3      | 4     | 5      | 6      | 7     | 8      | 9      |     |
| S     | 53.19  | 53.50                            | 53.28  | 53.28 | 53.19  | 53.40  | 53.97 | 53.28  | 53.19  |     |
| Fe    | 40.78  | 40.83                            | 40.47  | 40.45 | 38.77  | 38.73  | 38.26 | 41.20  | 39.10  |     |
| Cr    | 0.16   | 0.15                             | 0.18   | 0.18  | 0.20   | 0.11   | 0.13  | 0.15   | 0.14   |     |
| Co    | 0.13   | 0.09                             | 0.10   | 0.11  | 0.10   | 0.12   | 0.21  | 0.08   | 0.09   |     |
| Ni    | 5.72   | 5.42                             | 5.96   | 5.97  | 7.73   | 7.65   | 7.43  | 5.29   | 7.47   |     |
| Cu    | 0.01   | 0.00                             | 0.01   | 0.00  | 0.01   | 0.00   | 0.00  | 0.00   | 0.00   |     |
| Total | 100.0  | 100.0                            | 100.0  | 100.0 | 100.0  | 100.0  | 100.0 | 100.0  | 100.0  |     |
| wt%   |        | Core-2 (Outer Part) and Lamellae |        |       |        |        |       |        |        | Rim |
| N     | 1      | 2                                | 3      | 4     | 5      | 6      | 7     | 8      | 1      |     |
| S     | 32.97  | 33.33                            | 33.27  | 33.11 | 33.46  | 33.49  | 33.08 | 33.29  | 34.92  |     |
| Fe    | 27.22  | 27.16                            | 27.17  | 27.14 | 27.52  | 27.93  | 27.27 | 27.30  | 30.75  |     |
| Cr    | 0.03   | 0.04                             | 0.04   | 0.04  | 0.17   | 0.18   | 0.19  | 0.05   | 0.04   |     |
| Co    | 0.97   | 1.08                             | 0.95   | 0.90  | 0.50   | 0.72   | 0.55  | 0.97   | 0.06   |     |
| Ni    | 38.96  | 38.71                            | 38.68  | 38.69 | 38.64  | 37.94  | 38.61 | 38.64  | 1.09   |     |
| Cu    | 0.04   | 0.00                             | 0.00   | 0.03  | 0.00   | 0.04   | 0.00  | 0.02   | 33.38  |     |
| Total | 100.17 | 100.32                           | 100.12 | 99.90 | 100.29 | 100.30 | 99.71 | 100.27 | 100.23 |     |
| at%   |        | Core-2 (Outer Part) and Lamellae |        |       |        |        |       |        |        | Rim |
| N     | 1      | 2                                | 3      | 4     | 5      | 6      | 7     | 8      | 1      |     |
| S     | 46.81  | 47.16                            | 47.17  | 47.06 | 47.30  | 47.33  | 47.10 | 47.14  | 49.84  |     |
| Fe    | 22.19  | 22.06                            | 22.11  | 22.15 | 22.34  | 22.66  | 22.29 | 22.18  | 25.20  |     |
| Cr    | 0.02   | 0.04                             | 0.04   | 0.03  | 0.15   | 0.16   | 0.17  | 0.04   | 0.03   |     |
| Co    | 0.75   | 0.83                             | 0.73   | 0.69  | 0.38   | 0.55   | 0.43  | 0.75   | 0.05   |     |
| Ni    | 30.21  | 29.92                            | 29.94  | 30.04 | 29.83  | 29.28  | 30.02 | 29.88  | 0.85   |     |
| Cu    | 0.03   | 0.00                             | 0.00   | 0.02  | 0.00   | 0.03   | 0.00  | 0.01   | 24.03  |     |
| Total | 100.0  | 100.0                            | 100.0  | 100.0 | 100.0  | 100.0  | 100.0 | 100.0  | 100.0  |     |

Note: EMPA data from JEOL JXA-8100 electron microprobe. Analyzed by V.N. Korolyuk. Formula. Core-1:  $(\text{Fe,Ni})_{0.85-0.88}\text{S}$ ; Core-2 and lamellae:  $(\text{Fe,Ni})_{8.88-9.09}\text{S}_8$ ; rim:  $\text{Fe}_{1.01}\text{Ni}_{0.03}\text{Cu}_{0.96}\text{S}_2$ .

### 3.3. Micro-Raman Spectroscopy Data

To detect signs of diamond-forming media, the interface between diamond inclusion and olivine as well as a net of stress cracks around the diamond were analyzed using the micro-Raman spectroscopic technique. The low-intensity mode in the 3050–3140  $\text{cm}^{-1}$  interval with a peak at 3094  $\text{cm}^{-1}$  was observed in three spectra out of ten. According to [32], this value corresponds to the vibrational modes of aromatic or olefinic compounds (Figure 4, Spectrum b). Those spectra were taken from the contact of olivine with diamond directly. Analyses of the cracks far from the diamond showed the forsterite modes only.

### 3.4. Re-Os Isotope Data

The Re-Os isotope data were collected ablating the central part of the sulfide. The results of the LAM-MC-ICPMS are given in Table 4. The Os concentration is 731 ppm, and the  $^{187}\text{Re}/^{188}\text{Os}$  ratio 0.05261 is well below the threshold (1.18) for which a reliable

correction can be carried out [21]. Modeling by Griffin et al. [33] also suggested that sulfides with  $^{187}\text{Re}/^{188}\text{Os} < 0.07$  are unlikely to have been disturbed by any metasomatic events. The TMA calculated using model parameters of Shirey and Walker [34] yields  $3.58 \pm 0.03$  Ga, while the TRD model age is  $3.15 \pm 0.03$  Ga (considering only the analytical uncertainties on  $^{187}\text{Os}/^{188}\text{Os}$  and  $^{187}\text{Re}/^{188}\text{Os}$ ).

**Table 4.** Re-Os isotope data for sulfide. 1—characteristics and modeling method; 2—data and estimated age; 3—error.

| 1                                       | 2        | 3        |
|---|----------|----------|
| Os                                      | 731 ppm  |          |
| $^{187}\text{Re}/^{188}\text{Os}$       | 0.05261  | 0.00039  |
| $^{187}\text{Os}/^{188}\text{Os}$       | 0.105736 | 0.000045 |
| $^{187}\text{Os}/^{188}\text{Os}_{360}$ | 0.105419 |          |
| $\text{Y Os}_{360}$                     | −17.1    |          |
| T (MA)                                  | 3.58     | 0.03     |
| T (RD)360                               | 3.15     | 0.03     |

Note: LAM-MC-ICPMS data. Analyzed by N.J. Pearson. T (MA) model parameters from [34], where MA is model age. T(RD)360—RD denotes Re depletion age, calculated from initial Os isotopic ratio at 360 Ma assuming Re/Os ratio = 0.  $\text{Y Os}_{360} = ((^{187}\text{Os}/^{188}\text{Os}_{\text{SAMPLE}} / ^{187}\text{Os}/^{188}\text{Os}_{\text{MANTLE}}) - 1) \times 100$  [35].

#### 4. Discussion

The compositions of mineral and fluid inclusions in diamonds [25,36–40] indicate the leading role of carbonatite metasomatism in diamond formation [41]. It was suggested, e.g., [42–44], that carbon came with mobile low-viscosity carbonatite melts percolating through rocks. In our case, however, the diamond octahedron with visible signs of resorption (Figure 3d) is set into the core of an olivine grain rather than in interstitials or cracks. Therefore, the included diamond must have another formation history. The elemental maps and composition data presented above of different olivine sections exclude the scenario of metasomatic diamond catching by olivine with late recrystallization of new-generation olivine near the diamond inclusion. It apparently is protogenetic and crystallized earlier than the host olivine at a high temperature, possibly and presumably from a carbon-bearing silicate melt. The generation conditions and compositions of similar melts were inferred from experiments with the respective systems and PT parameters [44]. Specifically, the solidus in the peridotite-C-O-H-fluid system, at ~6 GPa and an oxygen fugacity of the IW buffer, was shown to be about 1400 °C [45], or 200–250 °C higher than the Archean geotherm at this depth [46]. According to [47], metasomatism and diamond formation began shortly after cratonic lithosphere stabilization. Note that the diamond inclusion we found had crystallized long before most of the diamonds produced by metasomatic reactions of carbonatite melts with depleted peridotite, which already cooled down to the Middle Archean cratonic geotherm at depths within the diamond stability field.

Alternatively, considering the presence of sulfide inclusion in the same olivine grain where the diamond was found and the common occurrence of sulfide inclusions in diamond and its satellites, e.g., [2,30,48–50], the crystallization of diamond with a sulfide melt participation could not be ignored.

Although sulfide inclusions are frequently found in diamonds, some researchers interpret them to be xenogenic [43,51]. According to their experimental results, the FeS–NiS–CuS–K<sub>2</sub>S tetrahedron is settled beyond the conventional boundary of complete liquid immiscibility with the diamond-forming carbonate–silicate growth medium. However, the experiments on diamond crystallization in the Fe–S–C system with 5 wt% sulfur at the lowest pressures and temperatures of diamond synthesis and growth (5.5 GPa and  $1350 \pm 25$  °C) have shown that diamond can also grow from iron–sulfide melts [52]. Spetsius and Taylor [17] likewise admitted a possible genetic linkage between sulfides and diamonds. The intergrowths of sulfides and microdiamonds in zones of intense treatment of eclogite xenolith were observed [53].



During diamond synthesis experiments in Fe–Ni–S–C and Fe–Co–S–C systems, metastable graphite was observed [54,55]. Preferable crystallization of graphite at low PT in the pyrrhotite–pentlandite system was also observed in earlier experiments [56]. The reconstructed original composition of sulfide inclusion in olivine that we found corresponds to monosulfide solid solution or mss (troilite, according to S:Me) with 19.15 wt% Ni, about 6 wt% Cu, less than 0.5 wt% Co, and 0.1 wt% Cr. Therefore, we deal with the Fe–Ni–Cu–Co–(Cr)–S–C system. Graphite here was detected neither with diamond nor with sulfide, nor existing as a separate enclosed phase. According to Palyanov et al. [56], diamond may crystallize from sulfide melt at a pressure of 7.5 GPa and a temperature  $\geq 1600$  °C; however, sulfide melts play a minor role in experiments of diamond formation in comparison with the other possible media, such as carbonate, e.g., [57], carbonate–chloride [58], C–O–H fluid [59,60], and carbonate–silicate–C–O–H fluid [61] systems. At the same time, the authors noted that the natural environment of diamond formation is more complex, contains fluids, and probably is associated with redox reactions. Therefore, sulfides can act as reducing agents in the process of diamond formation from carbonate [62]. In [63], the mechanism of such a formation was shown. The sulfide composition changed during the reaction. At a temperature lower than pyrrhotite liquidus, the sulfide stoichiometry was  $\text{Fe}_{0.85}\text{S}$ . It should be noted that iron deficiency is also observed in the inner core (central part) of our sulfide (formula  $(\text{Fe,Ni})_{0.85-0.88}\text{S}$ ).

The Archean Re–Os model ages (TMA  $3.58 \pm 0.03$  Ga and TRD  $3.15 \pm 0.03$  Ga) of the studied sulfide inclusion are in good agreement with previous geochronological studies of the Siberian crustal and mantle rocks. The Re–Os model age (TMA) calculations assume single-stage closed-system evolution. The Re depletion age (TRD) defines a minimum possible age for the Os in the sulfide but does not define the age of the sulfide crystallization. Re depletion model ages are usually applied when Re contents are suspected to be modified by metasomatic processes [64]. Both ages fall in the range of 3.6–2.8 Ga of the Archean formation of the lithosphere of the Siberian craton. Based on Re–Os data of mantle xenoliths and xenocrysts from the Udachnaya pipe, it was shown that a thick Archean lithospheric mantle beneath the Siberian craton had already been formed in the early Archean time [12,13,33,35]. A detailed mineralogical study of the megacrystalline peridotites with subcalcic pyropes (some of them are diamond-bearing) revealed their similarity to the mineralogy and chemical composition of the diamond inclusions in Siberian kimberlites [9,11–13,26]. These observations allow us to suppose that the megacrystalline peridotites (harzburgites or dunites) with subcalcic pyropes or chromite are the host rocks of the Siberian peridotitic diamonds. Re–Os dating of the megacrystalline peridotites with subcalcic pyropes gave two TRD age groups,  $\sim 1.8$  Ga and 2.8–3.2 Ga, confirming that the thick diamondiferous lithosphere was formed in the Archean time [35]. Re–Os dating of the sulfide inclusions in xenocrystal mantle olivine from the Udachnaya pipe indicates that at least part of the lithospheric mantle beneath the Daldyn kimberlite field formed during the period 3–3.5 Ga [33].

The lithospheric mantle of the Siberian craton since the Archean had multiple episodes of mantle metasomatism—from Archean to very recent times prior to kimberlite eruption [12,13,35,65–71]. The studied sulfide is fully enclosed in the host olivine grain, and therefore, it might keep its original Re–Os isotope system undisturbed. However, it is well known that olivine is not resistant to shear deformations and quite easily breaks and recrystallizes. Thus, someone may potentially assume that the Re–Os isotope system might have been disturbed by any of these metasomatic events, which are usually accompanied by deformation of the host peridotite. The metasomatic alteration of primary highly reduced diamond-bearing peridotites [68] leads to oxidation of their primary mineralogy [72]. Garnet peridotites from the Udachnaya pipe are more oxidized than those of the Kaapvaal craton. Fluid specification of the Udachnaya garnet peridotites shows that water is the dominant fluid species ( $>50\%$ ), with the maximum ( $\geq 90\%$ ) in the depth range of 100–175 km and increasing methane fraction with a depth below the graphite/diamond transition boundary [23,73,74]. However, the high mg# of the host olivine (93.1), a low

$^{187}\text{Re}/^{188}\text{Os}$  ratio of 0.05261 in the sulfide, and findings of reduced aromatic or olefinic compounds near the diamond inclusion rather indicate that this sample was not disturbed by any oxidized metasomatic fluids. The sulfide grain is also lacking the djerfisherite rim, which is frequently found in Udachnaya mantle xenoliths and the appearance of which is a reliable indicator of interaction with kimberlitic fluids [75]. Based on this argumentation, we assume that the original Re-Os system of the sulfide was not disturbed, the TMA model age of  $3.58 \pm 0.03$  Ga (which accounts for Re in the model age calculation) is significant, and the TRD  $3.15 \pm 0.03$  Ga age defines a minimum possible age for the Os in this sulfide. The similarity of the sulfide inclusion Re-Os model ages to the oldest Re-Os ages from Siberian peridotite xenoliths indicates that (1) the studied diamond inclusion in olivine belongs to the earliest generation of diamonds in the Siberian cratonic lithosphere (3.5 Ga [76,77]), (2) the formation of diamonds in the depleted cratonic lithosphere starts immediately after the formation of the earliest lithosphere at  $\sim 3.6$  Ga.

## 5. Conclusions

1. The crystallization of the diamond inclusion that we found must have proceeded either from silicate melt, enriched with a carbonate component (carbon-bearing fluid), or proceeded from sulfide melt with dissolved carbon (Fe-Ni-Cu-Co-S-C melt).
2. Crystallization of the studied diamond occurred at temperatures at least 200–250 °C higher than for the crystallization of later metasomatic diamonds: in the case of silicate melt, at 1400 °C; in the case of sulfide melt, at 1600 °C.
3. The diamond we discovered is apparently the oldest to date. The age of the syngenetic inclusion of sulfide is estimated at  $\sim 3.6$  billion years.

**Author Contributions:** Conceptualization, N.P. and L.P.; investigation, L.P., V.M. and T.A.; resources, L.P., V.M. and T.A.; writing—original draft preparation, L.P. and V.M.; writing—review and editing, L.P.; visualization, L.P. and T.A.; supervision, L.P.; project administration, L.P.; funding acquisition, N.P. and L.P. All authors have read and agreed to the published version of the manuscript.

**Funding:** L. Pokhilenko is grateful for the support of the Russian Science Foundation (project number 21-17-00082). The Re-Os isotopic studies were investigated by V.M. with support from the Russian Science Foundation (project number 22-27-00724). N.P. acknowledges the support of the Russian Foundation for Basic Research (grant number 20-05-00662).

**Data Availability Statement:** Not applicable.

**Acknowledgments:** Most of the analytical work was carried out at the Analytical Center for Multi-element and Isotope Research of the Siberian Branch of the Russian Academy of Sciences and was undertaken on the state assignment of IGM SB RAS. We wish to thank our colleagues from IGM (Novosibirsk) for their assistance, especially V.N. Korolyuk for the EMPA work, M.V. Khlestov for the TESCAN work, and S.Z. Smirnov and E. Nikolenko for photographing the diamond and sulfide inclusions. Special thanks to N.J. Pearson for the Re-Os isotope analysis of the sulfide inclusion. The authors express their sincere gratitude to W.L. Griffin for correction and editing the first English translation of the manuscript. We also thank the MDPI Reviewers and Academic Editors for their attention to our research, the corrections and comments made, and, most importantly, their personal time. Thanks to all Minerals Editorial Office staff for friendly and attentive attitude while working on the article.

**Conflicts of Interest:** Authors declare no conflict of interest.

## References

1. Prinz, M.; Manson, D.V.; Hlava, P.F.; Keil, K. Inclusions in diamonds: Garnet lherzolite and eclogite assemblages. *Phys. Chem. Earth* **1975**, *9*, 797–815. [[CrossRef](#)]
2. Efimova, E.S.; Sobolev, N.V.; Pospelova, L.N. Sulfide inclusions in diamond and their paragenesis features. *Rep. Russ. Mineral. Soc.* **1983**, *112*, 300–310. (In Russian)
3. Deines, P.; Harris, J.W. Sulfide inclusion chemistry and carbon isotopes of African diamonds. *Geochim. Cosmochim. Acta* **1995**, *59*, 3173–3188. [[CrossRef](#)]

4. Schulze, D.J.; Coopersmith, H.G.; Harte, B.; Pizzolato, L.A. Mineral inclusions in diamonds from the Kelsey Lake Mine, Colorado, USA: Depleted Archean mantle beneath the Proterozoic Yavapai province. *Geochim. Cosmochim. Acta* **2008**, *72*, 1685–1695. [[CrossRef](#)]
5. Jean, M.M.; Taylor, L.A.; Howarth, G.H.; Peslier, A.H.; Fedele, L.; Bodnar, R.J.; Guan, Y.; Doucet, L.S.; Ionov, D.A.; Logvinova, A.M.; et al. Olivine inclusions in Siberian diamonds and mantle xenoliths: Contrasting water and trace-element contents. *Lithos* **2016**, *265*, 31–41. [[CrossRef](#)]
6. Carvalho, L.D.V.; Schnellrath, J.; Medeiros, S.R. Mineral inclusions in diamonds from Chapada Diamantina, Bahia, Brazil: A Raman spectroscopic characterization. *REM Int. Eng. J.* **2018**, *71*, 27–35. [[CrossRef](#)]
7. Nestola, F.; Zaffiro, G.; Mazzucchelli, M.L.; Nimis, P.; Andreozzi, G.B.; Periotto, B.; Princivalle, F.; Lenaz, D.; Secco, L.; Pasqualetto, L.; et al. Diamond-inclusion system recording old deep lithosphere conditions at Udachnaya (Siberia). *Sci. Rep.* **2019**, *9*, 12586. [[CrossRef](#)]
8. Sobolev, N.V.; Logvinova, A.M.; Tomilenko, A.A.; Wirth, R.; Bul'bak, T.A.; Luk'yanova, L.I.; Fedorova, E.N.; Reutsky, V.N.; Efimova, E.S. Mineral and fluid inclusions in diamonds from the Urals placers, Russia: Evidence for solid molecular N<sub>2</sub> and hydrocarbons in fluid inclusions. *Geochim. Cosmochim. Acta* **2019**, *266*, 197–219. [[CrossRef](#)]
9. Pokhilenko, N.P.; Sobolev, N.V.; Lavrent'ev, Y.G. Xenoliths of diamondiferous ultramafic rocks from Yakutian kimberlites. In Proceedings of the II International Kimberlite Conference, Santa Fe, NM, USA, 3–7 October 1977. Available online: <https://archive.org/details/secondinternatio02inte> (accessed on 24 November 2022).
10. Ilupin, I.P.; Efimova, E.S.; Sobolev, N.V.; Usova, L.V.; Savrasov, D.I.; Kharkiv, A.D. Inclusions in diamond from diamondiferous dunite. *Dokl. Acad. Nauk SSSR* **1982**, *264*, 454–456.
11. Sobolev, N.V.; Pokhilenko, N.P.; Efimova, E.S. Xenoliths of diamondiferous peridotite in kimberlites and the origin of diamond. *Soviet Geol. Geophys.* **1984**, *25*, 63–80.
12. Pokhilenko, N.P.; Pearson, D.G.; Boyd, F.R.; Sobolev, N.V. Megacrystalline Dunites: Sources of Siberian Diamonds. In *Annual Report of Director Geophysical Laboratory*; Carnegie Institution: Washington, DC, USA, 1991; pp. 11–18.
13. Pokhilenko, N.P.; Sobolev, N.V.; Boyd, F.R.; Pearson, D.G.; Shimizu, N. Megacrystalline pyrope peridotites in the lithosphere of the Siberian platform: Mineralogy, geochemical peculiarities and the problem of their origin. *Russ. Geol. Geophys.* **1993**, *34*, 71–84.
14. Sobolev, N.V. *Deep-Seated Inclusions in Kimberlites and the Problem of the Composition of the Upper Mantle*; American Geological Union: Washington, DC, USA, 1977; 279p.
15. Garanin, V.K.; Zaborovskii, V.V.; Kudryavtseva, G.P.; Mikhailichenko, O.A.; Sobolev, N.V. Mineralogy of Diamondiferous Garnet Nodules from the Udachnaya Kimberlite (Yakutia). In Proceedings of the International Symposium Deep Subcontinental Lithosphere: Composition and Processes, Novosibirsk, Russia, 30 May–2 June 1988.
16. Barashkov, Y.P.; Zudin, N.G. The composition of garnets with diamond inclusions from the Krasnopresnenskaya kimberlite pipe (Yakutia). *Russ. Geol. Geophys.* **1997**, *38*, 353–357.
17. Spetsius, Z.V.; Taylor, L.A. *Diamonds of Siberia: Photographic Evidence for their Origin*; Tranquility Base Press: Lenoir City, TN, USA, 2008; 278p.
18. Howarth, G.H.; Sobolev, N.V.; Pernet-Fisher, J.F.; Ketcham, R.A.; Maisano, J.A.; Pokhilenko, L.N.; Taylor, D.; Taylor, L.A. 3-D X-ray tomography of diamondiferous mantle eclogite xenoliths, Siberia. *J. Asian Earth Sci.* **2015**, *101*, 39–67. [[CrossRef](#)]
19. Laz'ko, E.E.; Pokhilenko, N.P.; Lavrentiev, Y.G.; Usova, L.V. Compositions of mineral inclusions in olivines from the Udachnaya kimberlite (Yakutia). *Soviet Geol. Geophys.* **1976**, *17*, 107–112.
20. Kamenetsky, V.S.; Kamenetsky, M.B.; Sobolev, A.V.; Golovin, A.V.; Demouchy, S.; Faure, K.; Sharygin, V.V.; Kuzmin, D.V. Olivine in the Udachnaya-East Kimberlite (Yakutia, Russia): Types, Compositions and Origins. *J. Petrol.* **2008**, *49*, 823–839. [[CrossRef](#)]
21. Pearson, N.J.; Alard, O.; Griffin, W.L.; Jackson, S.E.; O'Reilly, S.Y. In situ measurement of Re–Os isotopes in mantle sulfides by laser ablation multicollector-inductively coupled plasma mass spectrometry: Analytical methods and preliminary results. *Geochim. Cosmochim. Acta* **2002**, *66*, 1037–1050. [[CrossRef](#)]
22. Alard, O.; Griffin, W.L.; Lorand, J.-P.; Jackson, S.E.; O'Reilly, S.Y. Non-chondritic distribution of the highly siderophile elements in mantle sulfides. *Nature* **2000**, *407*, 891–894. [[CrossRef](#)]
23. Griffin, W.L.; Powell, W.J.; Pearson, N.J.; O'Reilly, S.Y. GLITTER: Data reduction software for laser ablation ICP-MS. In *Laser Ablation ICP-MS in the Earth Sciences: Current Practices and Outstanding Issues*; Sylvester, P.J., Ed.; Mineralogical Association of Canada Short Course Series; Short Course 40; Mineralogical Association of Canada: Vancouver, BC, Canada, 2008; pp. 308–311.
24. Pokhilenko, L.N. The Fluid Regime of Lithospheric Mantle in the Siberian Craton (from Mantle Xenoliths in Kimberlites). Author's Abstract. Ph.D. Thesis, Institute of Geology & Mineralogy, Novosibirsk, Russia, 2006; 16p. (In Russian)
25. Sobolev, N.V.; Logvinova, A.M.; Zedgenizov, D.A.; Pokhilenko, N.P.; Malygina, E.V.; Kuzmin, D.V.; Sobolev, A.V. Petrogenetic significance of minor elements in olivines from diamonds and peridotite xenoliths from kimberlites of Yakutia. *Lithos* **2009**, *112*, 701–713. [[CrossRef](#)]
26. Pokhilenko, L.N.; Mal'kovets, V.G.; Kuz'min, D.V.; Pokhilenko, N.P. New Data on the Mineralogy of Megacrystalline Pyrope Peridotite from the Udachnaya Kimberlite Pipe, Siberian Craton, Yakutian Diamondiferous Province. *Dokl. Earth Sci.* **2014**, *454*, 179–184. [[CrossRef](#)]
27. Arndt, N.T.; Guitreau, M.; Boullier, A.-M.; Le Roex, A.; Tommasi, A.; Cordier, P.; Sobolev, A.V. Olivine, and the origin of kimberlite. *J. Petrol.* **2010**, *51*, 573–602. [[CrossRef](#)]

28. Donnelly, C.L.; Stachel, T.; Creighton, S.; Muehlenbachs, K.; Whiteford, S. Diamonds and their mineral inclusions from the A154 South pipe, Diavik Diamond Mine, Northwest territories, Canada. *Lithos* **2007**, *98*, 160–176. [[CrossRef](#)]
29. Sobolev, N.V.; Logvinova, A.M.; Zedgenizov, D.A.; Pokhilenko, N.P.; Kuzmin, D.V.; Sobolev, A.V. Olivine inclusions in Siberian diamonds: High-precision approach to minor elements. *Eur. J. Mineral.* **2008**, *20*, 305–315. [[CrossRef](#)]
30. Van Rythoven, A.D.; Schulze, D.J. In situ analysis of diamonds and their inclusions from the Diavik Mine, Northwest Territories, Canada: Mapping diamond growth. *Lithos* **2009**, *112*, 870–879. [[CrossRef](#)]
31. Shatsky, V.S.; Zedgenizov, D.A.; Ragozin, A.L.; Kalinina, V.V. Diamondiferous subcontinental lithospheric mantle of the northeastern Siberian Craton: Evidence from mineral inclusions in alluvial diamonds. *Gondwana Res.* **2015**, *28*, 106–120. [[CrossRef](#)]
32. Socrates, G. *Infrared and Raman Characteristic Group Frequencies: Tables and Charts*, 3rd ed.; John Wiley and Sons, Ltd.: Chichester, UK, 2004; 368p.
33. Griffin, W.L.; Spetsius, Z.V.; Pearson, N.J.; O'Reilly, S.Y. In situ Re–Os analysis of sulfide inclusions in kimberlitic olivine: New constraints on depletion events in the Siberian lithospheric mantle. *Geochem. Geophys. Geosyst.* **2002**, *3*, 1069. [[CrossRef](#)]
34. Shirey, S.B.; Walker, R.J. The Re–Os isotope system in cosmochemistry and high-temperature geochemistry. *Annu. Rev. Earth Planet. Sci.* **1998**, *26*, 423–500. [[CrossRef](#)]
35. Pearson, D.G.; Shirey, S.B.; Carlson, R.W.; Boyd, F.R.; Pokhilenko, N.P.; Shimizu, N. Re–Os, Sm–Nd, and Rb–Sr isotope evidence for thick Archaean lithospheric mantle beneath the Siberian craton modified by multistage metasomatism. *Geochim. Cosmochim. Acta* **1995**, *59*, 959–977. [[CrossRef](#)]
36. Klein-Ben David, O.; Logvinova, A.M.; Schrauder, M.; Spetius, Z.V.; Weiss, Y.; Hauri, E.H.; Kaminsky, F.V.; Sobolev, N.V.; Navon, O. High-Mg carbonatitic microinclusions in some Yakutian diamonds—A new type of diamond-forming fluid. *Lithos* **2009**, *112*, 648–659. [[CrossRef](#)]
37. Klein-BenDavid, O.; Pearson, D.G.; Nowell, G.M.; Ottley, C.; McNeill, J.C.R.; Logvinova, A.M.; Sobolev, N.V. The sources and time-integrated evolution of diamond-forming fluids—Trace elements and isotopic evidence. *Geochim. Cosmochim. Acta* **2014**, *125*, 146–169. [[CrossRef](#)]
38. Logvinova, A.M.; Wirth, R.; Fedorova, E.N.; Sobolev, N.V. Nanometre-sized mineral and fluid inclusions in cloudy Siberian diamonds: New insights on diamond formation. *Eur. J. Mineral.* **2008**, *20*, 317–331. [[CrossRef](#)]
39. Logvinova, A.M.; Wirth, R.; Tomilenko, A.A.; Afanasiev, V.P.; Sobolev, N.V. The phase composition of crystal-fluid nanoinclusions in alluvial diamonds in the northeastern Siberian Platform. *Russ. Geol. Geophys.* **2011**, *52*, 1286–1297. [[CrossRef](#)]
40. Zedgenizov, D.A.; Rege, S.; Griffin, W.L.; Kagi, H.; Shatsky, V.S. Composition of trapped fluids in cuboid fibrous diamonds from the Udachnaya kimberlite: LAM-ICPMS analysis. *Chem. Geol.* **2007**, *240*, 151–162. [[CrossRef](#)]
41. Pokhilenko, N.P.; Agashev, A.M.; Litasov, K.D.; Pokhilenko, L.N. Carbonatite metasomatism of peridotite lithospheric mantle: Implications for diamond formation and carbonatite-kimberlite magmatism. *Russ. Geol. Geophys.* **2015**, *56*, 280–295. [[CrossRef](#)]
42. Pal'yanov, Y.N.; Sokol, A.G.; Borzdov, Y.M.; Khokhryakov, A.F.; Sobolev, N.V. Diamond formation through carbonate-silicate interaction. *Am. Mineral.* **2002**, *87*, 1009–1013. [[CrossRef](#)]
43. Litvin, Y.A.; Bobrov, A.V.; Vasil'ev, P.G.; Okoemova, V.Y.; Kuzyura, A.V. Parental media of natural diamonds and primary mineral inclusions in them: Evidence from physicochemical experiment. *Geochem. Int.* **2012**, *50*, 726–759. [[CrossRef](#)]
44. Shirey, S.B.; Cartigny, P.; Frost, D.J.; Keshav, S.; Nestola, F.; Nimis, P.; Pearson, D.G.; Sobolev, N.V.; Walter, M.J. Diamonds and the geology of mantle carbon. *Rev. Mineral. Geochem.* **2013**, *75*, 355–421. [[CrossRef](#)]
45. Litasov, K.D. Physicochemical Conditions of Melting in the Mantle in the Presence of Volatiles (from Experimental Data). Ph.D. Thesis, Institute of Geology & Mineralogy, Novosibirsk, Russia, 2011; 35p. (In Russian)
46. Boyd, F.R.; Pokhilenko, N.P.; Pearson, D.G.; Mertzman, S.A.; Sobolev, N.V.; Finger, L.W. Composition of the Siberian cratonic mantle: Evidence from Udachnaya peridotite xenoliths. *Contrib. Mineral. Petrol.* **1997**, *128*, 228–246. [[CrossRef](#)]
47. Stachel, T.; Harris, J. The origin of cratonic diamonds—constraints from mineral inclusions. *Ore Geol. Rev.* **2008**, *34*, 5–32. [[CrossRef](#)]
48. Botkunov, A.I.; Garanin, V.K.; Gotovtsev, V.V.; Kudryavtseva, G.P. Sulfide inclusions in olivine from the Udachnaya kimberlite. *Dokl. Akad. Nauk SSSR* **1979**, *247*, 929–932. (In Russian)
49. Meyer, H.O.A. Inclusions in Diamond. In *Mantle Xenoliths*; Nixon, P.H., Ed.; John Wiley and Sons: Chichester, UK; New York, NY, USA, 1987; pp. 501–523.
50. Bulanova, G.P.; Spetsius, Z.V.; Leskova, N.V. *Sulfides in Diamonds and Xenoliths from Kimberlitic Pipes of Yakutia*; Nauka: Novosibirsk, Russia, 1990; 120p. (In Russian)
51. Shushkanova, A.V.; Litvin, Y.A. Experimental liquid immiscibility in sulphide-silicate pyrrhotite-garnet system at 7 GPa: Implication to origin of diamond and syngenetic inclusions. *Lithos* **2004**, *73*, 101.
52. Zhimulev, E.I.; Shein, M.A.; Pokhilenko, N.P. Crystallization of diamond in the system Fe-S-C. *Dokl. Earth Sci.* **2013**, *451*, 729–731. [[CrossRef](#)]
53. Spetsius, Z.V. The form, nature and conditions of partial melting of eclogites from the kimberlite pipes. *Vestn. MGU Geol.* **1980**, *4*, 101–105.
54. Chepurov, A.I.; Zhimulev, E.I.; Sonin, V.M.; Chepurov, A.A.; Pokhilenko, N.P. Crystallization of diamond in metal-sulfide melts. *Dokl. Earth Sci.* **2009**, *428*, 1139–1141. [[CrossRef](#)]
55. Zhimulev, E.I.; Chepurov, A.I.; Sinyakova, E.F.; Sonin, V.M.; Chepurov, A.A.; Pokhilenko, N.P. Diamond crystallization in the Fe-Co-S-C and Fe-Ni-S-C systems and the role of sulfide-metal melts in the genesis of diamond. *Geochem. Int.* **2012**, *50*, 205–216. [[CrossRef](#)]

56. Pal'yanov, Y.N.; Borzdov, Y.M.; Khokhryakov, A.F.; Kupriyanov, I.N.; Sobolev, N.V. Sulfide melts-graphite interaction at HPHT conditions: Implications for diamond genesis. *Earth. Planet. Sci. Lett.* **2006**, *250*, 269–280. [CrossRef]
57. Pal'yanov, Y.N.; Sokol, A.G.; Borzdov, Y.M.; Khokhryakov, A.F.; Shatsky, A.F.; Sobolev, N.V. The diamond growth from Li<sub>2</sub>CO<sub>3</sub>, Na<sub>2</sub>CO<sub>3</sub>, K<sub>2</sub>CO<sub>3</sub> and Cs<sub>2</sub>CO<sub>3</sub> solvent-catalysts at P = 7 GPa and T = 1700–1750 °C. *Diamond Relat. Mater.* **1999**, *8*, 1118–1124. [CrossRef]
58. Tomlinson, E.; Jones, A.; Milledge, J. High-pressure experimental growth of diamond using C–K<sub>2</sub>CO<sub>3</sub>–KCl as an analogue for Cl-bearing carbonate fluid. *Lithos* **2004**, *77*, 287–294. [CrossRef]
59. Akaishi, M.; Yamaoka, S. Crystallization of diamond from C–O–H fluids under high-pressure and high-temperature conditions. *J. Cryst. Growth* **2000**, *209*, 999–1003. [CrossRef]
60. Sokol, A.G.; Pal'yanov, Y.N.; Pal'yanova, G.A.; Khokhryakov, A.F.; Borzdov, Y.M. Diamond and graphite crystallization from C–O–H fluids under high pressure and high temperature conditions. *Diamond Relat. Mater.* **2001**, *10*, 2131–2136. [CrossRef]
61. Pal'yanov, Y.N.; Sokol, A.G.; Tomilenko, A.A.; Sobolev, N.V. Conditions of diamond formation through carbonate–silicate interaction. *Eur. J. Mineral.* **2005**, *2*, 207–214. [CrossRef]
62. Marx, P.C. Pyrrhotine and the origin of terrestrial diamonds. *Miner. Mag.* **1972**, *38*, 636–638. [CrossRef]
63. Pal'yanov, Y.N.; Borzdov, Y.M.; Bataleva, Y.V.; Sokol, A.G.; Pal'yanova, G.A.; Kupriyanov, I.N. Reducing role of sulfides and diamond formation in the Earth's mantle. *Earth. Planet. Sci. Lett.* **2007**, *260*, 242–256. [CrossRef]
64. Walker, R.; Carlson, R.; Shirey, S.; Boyd, F. Os, Sr, Nd, and Pb isotope systematics of southern African peridotite xenoliths and implications for the chemical evolution of the subcontinental mantle. *Geochim. Cosmochim. Acta* **1989**, *53*, 1583–1595. [CrossRef]
65. Pokhilenko, N.P.; Sobolev, N.V.; Kuligin, S.S.; Shimizu, N. Peculiarities of distribution of pyroxenite paragenesis garnets in Yakutian kimberlites and some aspects of the evolution of the Siberian craton lithospheric mantle. In Proceedings of the 7th International Kimberlite Conference, Cape Town, South Africa, 1–17 April 1998. [CrossRef]
66. Shimizu, N.; Sobolev, N.V. Young peridotitic diamonds from the Mir kimberlite pipe. *Nature* **1995**, *375*, 394–397. [CrossRef]
67. Shimizu, N.; Pokhilenko, N.P.; Boyd, F.R.; Pearson, D.G. Geochemical characteristics of mantle xenoliths from Udachnaya kimberlite pipe. *Geol. Geophys.* **1997**, *38*, 194–205. Available online: <https://repository.geologyscience.ru/handle/123456789/20596> (accessed on 24 November 2022).
68. Shimizu, N.; Pokhilenko, N.P.; Boyd, F.R.; Pearson, D.G. Trace element characteristics of garnet dunites/harzburgites, host rocks for Siberian peridotitic diamonds. In Proceedings of the 7th International Kimberlite Conference, Cape Town, South Africa, 1–17 April 1998. [CrossRef]
69. Malkovets, V.G.; Griffin, W.L.; O'Reilly, S.Y.; Wood, B.J. Diamond, subcalcic garnet, and mantle metasomatism: Kimberlite sampling patterns define the link. *Geology* **2007**, *35*, 339–342. [CrossRef]
70. Griffin, W.L.; Belousova, E.A.; O'Neill, C.; O'Reilly, S.Y.; Malkovets, V.; Pearson, N.J.; Spetsius, S.; Wilde, S.A. The world turns over: Hadean–Archean crust–mantle evolution. *Lithos* **2014**, *189*, 2–15. [CrossRef]
71. Howarth, G.H.; Barry, P.H.; Pernet-Fisher, J.F.; Baziotis, I.P.; Pokhilenko, N.P.; Pokhilenko, L.N.; Bodnar, R.J.; Taylor, L.A.; Agashev, A.M. Superplume metasomatism: Evidence from Siberian mantle xenoliths. *Lithos* **2014**, *184–187*, 209–224. [CrossRef]
72. McCammon, C.A.; Griffin, W.L.; Shee, S.R.; O'Neill, H.S.C. Oxidation during metasomatism in ultramafic xenoliths from the Wessellon kimberlite, South Africa: Implications for the survival of diamond. *Contrib. Mineral. Petrol. Contrib. Mineral. Petrol.* **2001**, *141*, 287–296. [CrossRef]
73. Goncharov, A.G.; Ionov, D.A.; Doucet, L.S.; Pokhilenko, L.N. Thermal state, oxygen fugacity and C–O–H fluid speciation in cratonic lithospheric mantle: New data on peridotite xenoliths from the Udachnaya kimberlite, Siberia. *Earth Planet. Sci. Lett.* **2012**, *357–358*, 99–110. [CrossRef]
74. Tomilenko, A.; Chepurov, A.; Pal'yanov, Y.; Pokhilenko, L.; Shebanin, A. Volatile components in the upper mantle (based on data on fluid inclusion studies). *Russ. Geol. Geophys.* **1997**, *38*, 276–285.
75. Sharygin, I.S.; Golovin, A.V.; Pokhilenko, N.P. Djerfisherite in xenoliths of sheared peridotite in the Udachnaya-East pipe (Yakutia): Origin and relationship with kimberlitic magmatism. *Russ. Geol. Geophys.* **2012**, *53*, 247–261. [CrossRef]
76. Pearson, D.G.; Shirey, S.B.; Bulanova, G.P.; Carlson, R.W.; Milledge, H.J. Re–Os isotope measurements of single sulfide inclusions in a Siberian diamond and its nitrogen aggregation systematics. *Geochim. Cosmochim. Acta* **1999**, *63*, 703–711. [CrossRef]
77. Pearson, D.G.; Bulanova, G.P.; Shirey, S.B.; Carlson, R.W.; Milledge, H.J.; Barashkov, Y.P. Re–Os isotope constraints on the ages of Siberian diamonds. *J. Conf. Abstr.* **2000**, *5*, 776.

**Disclaimer/Publisher's Note:** The statements, opinions and data contained in all publications are solely those of the individual author(s) and contributor(s) and not of MDPI and/or the editor(s). MDPI and/or the editor(s) disclaim responsibility for any injury to people or property resulting from any ideas, methods, instructions or products referred to in the content.